
TWO-STREAM UNET NETWORKS FOR SEMANTIC SEGMENTATION IN MEDICAL IMAGES

A PREPRINT

Xin Chen, Ke Ding

Intel Corp.
2200 Mission College Blvd
Santa Clara, CA 95054
(xin.chen, ke.ding)@intel.com

ABSTRACT

Recent advances of semantic image segmentation greatly benefit from deeper and larger Convolutional Neural Network (CNN) models. Compared to image segmentation in the wild, properties of both medical images themselves and of existing medical datasets hinder training deeper and larger models because of overfitting. To this end, we propose a novel two-stream UNET architecture for automatic end-to-end medical image segmentation, in which intensity value and gradient vector flow (GVF) are two inputs for each stream, respectively. We demonstrate that two-stream CNNs with more low-level features greatly benefit semantic segmentation for imperfect medical image datasets. Our proposed two-stream networks are trained and evaluated on the popular medical image segmentation benchmarks, and the results are competitive with the state of the art. The code will be released soon.

1 Introduction

As an important subfield of image segmentation, medical image segmentation is a challenging task which has received a significant amount of attention in both academia and industry [1, 2, 3, 4, 5, 6, 7, 8, 9]. Since emerging deep CNNs [10] and their application to image segmentation [11], the segmentation task has made a remarkable progress in recent years, which benefits from improving visual representations with deeper and larger of CNNs models [8, 12, 13]. However, compared to images in the wild, the deeper and larger models are limited to medical segmentation because of the following challenges [14, 15, 16, 17]:

1. **Properties of medical datasets.** Size of medical image datasets are tiny. Privacy of patient information and labelling cost restrict to build large scale image datasets. Also, due to clinical applications, the number of categories is small, in general less than five and even only one. As a result, on average, size of the medical datasets is only one tenth or less than that of natural images.
2. **Properties of medical images themselves.** There are two challenges to train deeper models on medical images. First, medical images have similar intensities of pixels. Second, some factors of medical acquisition such as sampling artifacts, spatial aliasing, and some of the dedicated noise of modalities cause the indistinct and disconnected boundary's structures.

Ronneberger *et al.* [18] develop a novel U-shape model of the encoder-decoder network architecture, named UNET, and it outperforms marginally on three small cell datasets. In the encoder-decoder networks, skip connections have proved that they play a key role to recover fine-grained details of the target images. Therefore, in order to aggregate fine-grained information efficiently and effectively from different layers, Zhou *et al.* UNET++ [19], in which the topology of skip connections is redesigned. The advantage of the UNET++ architecture is that the models gradually aggregate features across the networks both horizontally and vertically.

Given properties of the medical images, a well-know assumption is that much information that are fused appropriately is an effective way to improve segmentation results rather than heavily depending on recovering from one feature map [20]. Take the EM segmentation task [21] for example, in [18] and [22], besides accuracy improvement from better CNNs models side, the post-processing step, combining sliding window and voting rule on overlay areas, also contributes greatly to increase the accuracy. As a result, *a question arises: can we design a new architecture, in which multiple low-level features are fed into CNNs models and they can work on these multiple features?*

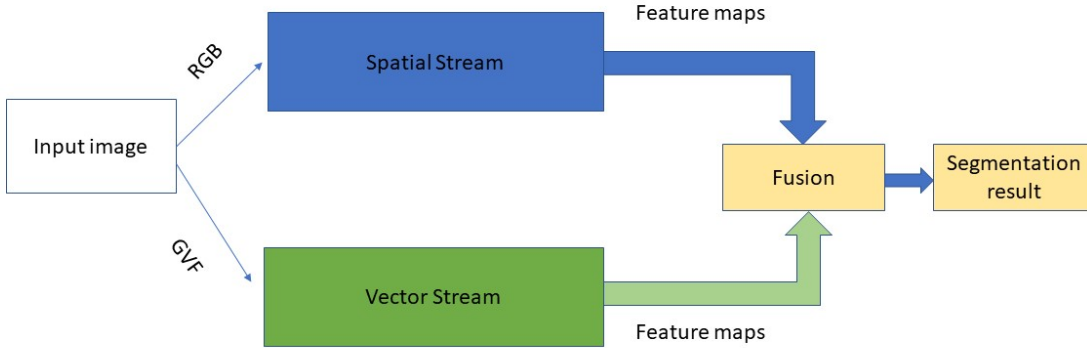


Figure 1: Visualization of our proposed two-stream UNET networks. We feed RGB (3-channel) or gray-level (1-channel) values into the spatial stream (blue) and corresponding stacked GVF fields to the vector stream (green). The backbone we take basic UNET model [18]. The outputs of each stream is $64 \times height \times width$. After the fusion layer, the output is $N \times height \times width$. N is number of classes. In the fusion layer, we took 1×1 convolutional kernel.

Inspired by two-stream hypothesis of human vision [23, 24] and state-of-the-art (SOTA) of action recognition in videos using two-stream networks [23], we propose a novel two-stream CNNs architecture for semantic segmentation in medical images, which incorporates spatial and vector field networks by introducing gradient vector flow (GVF) [25] as the input of the vector field network, for semantic segmentation in medical images. The backbone of each stream network of our two-stream networks is basic UNET [18] that is one of most popular CNNs architectures and is hypothesized that it is hard to beat if the corresponding pipeline is designed adequately [20]. The final fusion layer takes convolution fusion with 1×1 convolution kernel.

Our main contribution is to propose a novel two-stream UNET architecture to end-to-end learn for automatic segmentation in medical images. The two-stream networks consist of spatial and vector field networks, one is referred to as *spatial stream (SS)* and the other is referred to as *vector stream (VS)*. Our proposed model architecture is visualized in Figure. 1. The input of the spatial stream is intensity value of the pixels, either RGB or grayscale-level, and the input of the vector field one is gradient vector flow (GVF), 2-channel, as the input of the vector field network. GVF is considered as one of best low-level pixel-wise features and greatly improves original active contour model (Snake) [26] acting as a new external force [27].

To the best knowledge, our proposed tow-stream UNET is first two-stream networks for end-to-end learn to segment in all kinds of medical images. Through introducing GVF to VS, the models to learn an object (an pixel) how to moving to contours. Then our models reason positions of the contours. In turns, the two-stream networks successfully handle the segmentation task. Obviously, our work can be easily extended to other computer vision tasks, for example object detection, instance segmentation and so on.

Our experimental results demonstrate that: (1) Our proposed two-stream UNET model marginally improves UNET and substantially outperforms other SOTA UNET variants. (2): The two-stream model attains competitive results compared to well-known networks such as vision transformer (ViT) while requiring substantially fewer computational resources to train and inference.

2 Related work

There is an extensive literature on UNET and its variants, but here we mention just a few relevant papers on UNET architecture and and two-stream networks relative to image segmentation. Some surveys and relative works are found in [28, 29, 30, 31], and recently developed approaches are presented in the various challenges hold at annual MICCAI meetings¹.

In image segmentation task, most of existing two-stream networks aim to solve not enough labelling problems, for example different domain adaption [32], pseudo labeling with mutual attention network [33]. Hu *et al.* address a fully convolution two-stream network for interactive segmentation, which has a two-stream late fusion network (TSLFN) and a multi-scale refining network (MSRN). TSLFN predicts the foreground with a reduced resolution, and MSRN

¹<http://www.miccai.org/>

predicts the foreground at full resolution. Then both are fused for final result. One input is RGB data and the other is the minimum Euclidean distance between pixels and the user click. The inherited problem of interactive approaches is that the predictions heavily rely on the quality of user clicks. Moreover, the whole process is involved by users.

In UNET++ [34, 22], besides redesigning skip connections which flexibly fuse features in decoders, deep supervision is utilized for improving model training. UNET++ models fuse image features across the network instead of the same-scale features in U-net. Combining with deep supervision, UNET++ models outperform basic UNET averagely. However, considering low content of medical images, CNNs model represent less visual features of medical images than natural images.

We notice that in the past two years nnUNET (no-new-UNet) [20] has outperformed state-of-the-art (SOTA) architectures in the Medical Decathlon Challenge [35], then has set new benchmarks in more datasets. First, nnUNET takes a well-known hypothesis that basic UNET is hard to beat. This hypothesis theoretically supports why the basic UNET is well-suited for our two-stream networks for image segmentation. Second, nnUNET comprises of ten different datasets using an ensemble of the same U-Net architecture with an automated pipeline comprising of pre-processing, data augmentation and post-processing. nnUNET's time cost is expensive in both training and inference because nnUNET requires more than one model in inference. Also, the nnUNET model is not good at small objects and noise edges because there are resize operations with bi-linear interpolation during training.

Our work focuses on model architecture. We, therefore, majorly discuss UNET architecture and related architecture efforts such as UNET++. At the same time, we believe that our proposed two-stream UNET networks can improve as well if they will be a part of nnUNET framework. Also, although we only discuss 2D segmentation in this paper, it is easy to extend our work to 3D cases.

3 GVF, two-Stream networks and image segmentation

Two-stream networks demand for spatial and temporal components for learning spatial and temporal features. In this section, first of all, we introduce how two-stream networks are inspired by the two-stream hypothesis of human vision. Then we explain the relationship between GVF and pixel moving to the boundaries, and finally we discuss why two-stream networks can be used for image segmentation.

3.1 Two-stream hypothesis of human vision and action recognition

In terms of two-streams hypothesis [36, 24], the human visual cortex contains two streams (pathways): a ventral stream and a dorsal stream. The ventral stream reasons about object identity (object recognition), and the dorsal stream reasons about spatial relationships without regard for semantics (motion analysis). Therefore, in action recognition [23, 37] and other tasks in videos such as semantic robotic grasping [38], one stream is trained to learn spatial features and the other stream is trained to learn temporal features.

For two-stream networks for action recognition in videos, two inputs of the networks are naturally from RGB value of each frame and optical flow computed from adjacent frames [39, 40]. It is clear that the spatial stream acting as the ventral stream for learning spatial information from RGB data of each frame and temporal stream acting as dorsal stream for learning motion patterns in videos from optical flow.

For two-stream networks for image segmentation, the questions are *what can be fed into two-stream network for be trained and why two-stream networks for segmentation task?* The following two subsections will answer them.

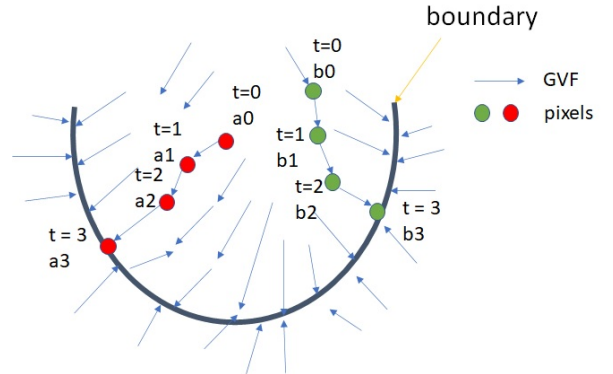


Figure 2: Visualization of relation between GVF and pixel motion analysis. The blue denotes GVF and red circle object is a pixel. Under the GVF, the object moves to edges step by step. For pixel a (red) will move from $a_0 \rightarrow a_1 \rightarrow a_2 \rightarrow a_3$ at time t_0, t_1, t_2, t_3 , and pixel b (green) will move from $b_0 \rightarrow b_1 \rightarrow b_2 \rightarrow b_3$ at time t_0, t_1, t_2, t_3 . a_3 and b_3 are pixels of the boundary.

3.2 GVF and two-stream networks

Background of GVF. GVF is the vector field that is produced by a process that smooths and diffuses an input vector field. It is usually used to create a vector field from images that points to object edges² from a distance [27]. The GVF is given by $\mathbf{V}(x, y) = [u(x, y), v(x, y)]$ at position (x, y) of an image. In this paper, we focus on CNNs and image segmentation, and more details of the GVF’s mathematical theory and computational solutions can be seen in [25, 27].

Why GVF is a well-suitable for two-stream architecture? According to Newton’s second law, motion patterns associate with forces that push the objects along with the direction of the force. We consider each pixel of an image is a component of an object. As shown in Figure. 2, pixels will move from the current position to the boundaries of the objects step by step under the GVF. The objective of image segmentation is to find the boundaries of the objects. As a result, GVF patterns represent how components move to the boundary of the object. Consequently, features from GVF infer to the boundaries in images.

For example, as shown in Figure. 2, given two objects, A (red) and B (green), we can imagine that the “A” object moves from position a_0, a_1, a_2, a_3 and stop in a_2 because a_3 is located in boundary. The same as object “B”.

3.3 Two-stream networks and image segmentation

If we consider semantic segmentation as pixel moving to boundary task, the VS is trained to learn how pixels move to the object boundary, and the SS is train to learn to recognize objects. It is obvious that it is an exact process of the image semantic segmentation task. As a consequence, two-stream networks are suitable to image segmentation.

There are two major reasons that two-stream networks are well-suited for medical image segmentation: (1) Each objects (organs) in medical images have their-own shape. and (2) The relationship among the location of the objects are fixed. There are some good patterns in GVF that offer visual features to be learned in VS for segmenting.

4 Methodology

We now present our approach for semantic segmentation in medical images. Specifically, we first address the basic architecture of our spatial and vector field feature extractors. Then we detail our fusion method with the convolution. Finally, we discuss our idea of losses function in our training.

4.1 Spatial and vector field feature extractor

UNET has shown that it is one of the powerful CNNs for learning visual representation in medical tasks. In our two-stream networks, we use the same network architecture excluding the last output layer of basic UNET developed in [18] as our spatial and vector field feature extractors, respectively. More details of UNET architecture can be seen in [18]. The total of UNET has 23 convolutional layers including final convolutional layer with 1×1 convolution. Both steams in our architecture have 22 convolutional layers and the channels of outputs are 64. In the kernel size of both extractors are 3×3 , stride is 1.

4.2 Two-stream Networks

In this subsection, we extend the basic UNET to two-stream UNET networks by adding a similar architecture but with GVF as the input. Figure 1 shows the main architecture of our proposed two-stream UNET networks.

There are four major techniques to fuse multiple feature maps [41]: sum fusion, max fusion, concatenation fusion, and convolution fusion. In our experiments, all of them can be used in our two-stream networks and improve the performances. In average, convolution fusion is better than others. Therefore, we use convolution fusion in this paper.

Given two feature maps, spatial feature maps \mathbf{X}^s and vector field features, \mathbf{X}^v , and they are concatenated firstly by:

$$y^{cat} = f^{cat}(\mathbf{X}^s, \mathbf{X}^v) \quad (1)$$

where f^{cat} is a concatenation operator and stacks two features maps along the channel dimension. Following it, a learnable of filter $\mathbf{f} \in \mathbb{R}^{M \times N}$ and biases $b \in \mathbb{R}^N$ is appended:

$$y^{conv} = y^{cat} * \mathbf{f} + b \quad (2)$$

²In image processing and computer vision, there are small differences among definitions of edge, contour, boundary. In this paper, we don’t strictly distinguish among them. If don’t mention, all of them mean the boundary of an object.

where $*$ denotes convolution, M denotes the sum number of channels of spatial and vector streams and N denotes the number of output channels. Filter f provides a flexible approach to project the channel dimension from M to N with weighted combining of outputs of the two streams.

4.3 Complete loss functions

In order to balance contributions of different losses during training, we train our networks with a weighed sum of dice and binary cross-entropy loss:

$$L_{total} = \alpha L_{dice} + (1 - \alpha) L_{bce} \quad (3)$$

where $\alpha \in [0, 1]$, and was estimated by

$$\alpha \propto \frac{\nabla L_{bce}}{\nabla L_{bce} + \nabla L_{dice}} \quad (4)$$

where ∇ is a gradient operator. In our experiments, we calculate gradient of losses in two epochs.

5 Experiment

5.1 Dataset

This section details the three widely-used datasets that we evaluate our approach in this paper and our experiment settings.

Electron Microscopy (EM) [21] The dataset consists of 30 images (512×512), and was EM segmentation challenge as a part of IEEE International Symposium on Biomedical Imaging (ISBI) 2012. The labeled images are split into training (24 images), validation (3 images), and test (3 images) datasets.

Automated cardiac diagnosis challenge (ACDC) [42] The ACDC challenge collects exams from different patients acquired from MRI scanners. Each patient scan is manually annotated with ground truth for left ventricle (LV), right ventricle (RV) and myocardium (MYO). These MRI images are randomly split to of 70 training cases (1930 axial slices), 10 cases for validation and 20 for testing.

Nuclei [43] The dataset is from the Data Science Bowl 2018 segmentation challenge and consists of 670 segmented nuclei images from different modalities. Images are randomly split into a training set (50%), a validation set (20%), and a test set (30%).

5.2 Experiment setting

We implemented the two-stream UNET networks in PyTorch 1.8 [44]. Implementation of UNET backbone is from ³ and implementation of GVF is from ⁴. In computation of GVF, the parameter μ , which is the GVF regularization coefficient, was set as 0.2, and the number of iteration of computation was set as 80. All our experiments were conducted on a system with a Nvidia Tesla V100 cards with 32G memory. Our models were trained on one GPU card. The operation system is Ubuntu 20.10.

6 Evaluation and results

In this section, we first discuss different evaluation methods. Then we compared our results to some of SOTA mehtods on three popular datasets, EM, Nuclei and ACDC datasets. The images of these dataset are acquired from MRI, CT, and rightfield VS fluorescence. Our results are competitive with the SOTA.

6.1 Evaluation

Most of previous works in EM and Nuclei datasets [18, 19], the predictions are aggregated across patches by voting in the overlapping areas. For instance, both SOTA results EM dataset reported from [18, 19], the images are extracted to

³<https://github.com/milesial/Pytorch-UNet>

⁴<https://github.com/Christophe-Foyer/GVF-Python>

Table 1: Semantic segmentation results measured by IOU (mean \pm s.d.%) on EM dataset for UNET, UNET++ and our approach. The results of UNET and UNET++ were in [19]. Both of them are with aggregation with voting on overlaps. Our results are directly predicted from two-stream models without post-processing. The best results are highlighted with bold. The same as others, for our approach, we have performed 20 independent trials.

	UNET [18]	UNET++ [19]	Ours
IOU	86.83 \pm 0.43	88.92 \pm 0.14	89.12 \pm0.18

Table 2: Semantic segmentation results measured by IOU on ADAC dataset. The results of others were in [45]. The top two methods in the Table 2 are UNET variant models, and others are ViT-based methods. The best results are highlighted with bold.

Method	Average DSC(%)	RV	MYO	LV
R50 UNET [46]	87.60	84.62	84.52	93.68
R50 AttnUNET [46]	86.90	83.27	84.33	93.53
ViT-CUP [45]	83.41	80.93	78.12	91.17
R50 ViT [46]	86.19	82.51	83.01	93.05
TransUNET [46]	89.71	86.67	87.27	95.18
Swin-UNET[46]	88.07	85.77	84.42	94.03
MT-UNET[45]	90.43	86.64	89.04	95.62
Ours	90.90	88.62	88.72	95.37

96 \times 96 patches with half of patch size overlaps. The final results are the aggregation with different patches with voting rule.

It is entirely reasonable to use post-process techniques to improve results and evaluate them for medical applications because medical image segmentation aims at aiding clinical applications. However, a big disadvantage of this type of evaluation is that the improvements of the approaches cannot figure out which parts (models and post-processing) attribute to and how much improvements respectively. In particular for model architecture work, the evaluation on these predictions is not effective because of the model performance is not clear.

Although some of results of previous works listed in this paper are still with post-processing such as EM dataset, our predictions are the models predictions without post-processing step. Even so, our proposed two-stream UNET networks have achieved SOTA in three datasets.

In this paper, we measure our method with either intersection-over-union (IoU), also known as the Jaccard index, or Dice score (DSC). In order to compare the previous works, which type of metrics was reported depends on that of the previous work results.

6.2 Experiment results

Results on Electron Microscopy (EM) dataset For training phase, the images (512 \times 512) was cut to 96 \times 96 patches with half of the patches size overlaps via sliding windows. For our inference phase, the images (512 \times 512) was cut to 96 \times 96 patches without overlaps. During training, the data augmentation methods that we took were image rotation, vertical and horizontal clips. The optimizer was ADAM optimizer, the learning rating is 0.0003, and batch size is 64. The total training epochs are 90 with early stopping. The losses function is weighted BCE and dice losses in Eq 3. The parameter α was set as 0.3. We trained our models from scratch. The training codebase that we revised for our two-stream networks training was from 3 .

As shown in Table 1, compared to two benchmarks, UNET and UNET++ at the same settings, our approach has achieved the best performance. It shows that two-stream UNET networks are effective architecture to learn features of spatial and GVF domains.

Results on ACDC dataset. For both training and inference phases, the resolution of the input images is 224 \times 224. During training, the data augmentation methods that we took were image rotation, vertical and horizontal clips. The optimizer was ADAM optimizer, the learning rating is 0.0003, and batch size is 12. The total training epochs are 90

Table 3: Semantic segmentation results measured by IOU (mean \pm s.d.%) on Nuclei dataset for UNET, UNET++, UNET++DS and our approach. UNET++DS denotes UNET++ with deep supervision during training. The results of others were in [6], last access on May 1, 2022. The best results are highlighted with bold. For our approach, we have performed 10 independent trials.

	UNET	UNET++	UNET++ DS	Ours
IOU(%)	83.9	84.2	84.3	84.6 \pm 0.01

with early stopping. The loss function is weighted CE and dice losses. The parameter α was set as 0.5. We trained our models from scratch. The training codebase that we revised for our two-stream networks training was from ⁵.

As shown in Table 2, our approach has achieved top 1 results in average results of three categories and RV task, and ranks second in MYO and LV segmentation. Furthermore, ours outperform marginally other CNNs methods at all in all segmentation tasks. Since the results of the same models on ADAC datasets reported in different papers are not exactly same, in order to avoid confusion, the results that we list in the Table 2 is from the latest paper [45].

Results Nuclei dataset For both training and inference phases, the resolution of the input images is 96×96 . During training, the data augmentation methods that we took were image rotation, vertical and horizontal clips. The optimizer was ADAM optimizer, the learning rate is 0.0003, and batch size is 16. The total training epochs are 90 with early stopping. The loss was Lovász-softmax loss [47]. The reason that we used the Lovász-softmax loss that beside is designed for image segmentation and a better in the task, we also evaluated our two-stream networks with different losses. The parameter α was set as 0.5. We trained our models from scratch. The training codebase that we revised for our two-stream networks training was from ⁶.

As shown in Table 3, ours are better than the results of UNET, UNET++ and UNET++ with deep supervision training. It points out that our two-stream UNET networks are robust, meaning they can be successfully trained in variety of situations, for example ours outperform UNET and UNET++ on different kinds of losses.

6.3 Limitations

As our proposed two-stream UNET networks are designed for medical image datasets, in which the size of dataset is tiny. We will apply the models to more big datasets to compare his performance to deeper models such as ViT-based models. In medical images, the number of categories are small and the objects (organs) have a fixed shape. What is more, the organs have the fixed position, meaning the location relationship among objects in medical images are fixed as well. These lead to GVF of medical images have good patterns. On the other hand, these properties of natural images are weaker. As a result, it will undermine the results of two-stream network for image segmentation in the wild.

7 Conclusion and future work

In this work we propose a novel two-stream UNET networks, which incorporates separate spatial and vector streams, for semantic segmentation in medical images. The backbone of both streams is UNET architecture. In perspective of motion, GVF indicates that the pixels of an images moves to the boundary of an object that the pixels belongs to. In term of motion analysis, the models can find the boundaries of the objects. As a consequence, two-stream networks are successfully trained on RGB input and GVF input that is calculated from RGB data. Extensive experiments validate the effectiveness of our proposed approach on semantic segmentation in medical images.

Aside from SOTA results on three challenging datasets, our approach also retains an attractive open scheme. There are two directions for future work are as followings:

1. Combining with other existing modules such as attention module, which have shown that models with attention have improved model training in medical image segmentation [48, 49]. We believe that attention module will offer an effective way to improve two-stream UNET networks for medical image segmentation.
2. The other way is to combine with some data pre-processing for improving training data quality, such as nnUNET. nnUNet has exhibited that the models benefited from better training data. Given CNNs are the data-driven method, high quality data will definitely improve the performance of CNNs models including our approach.

⁵<https://github.com/dootmaan/mt-unet>

⁶<https://github.com/4uiiurz1/pytorch-nested-unet>

References

- [1] Dzung L Pham, Chenyang Xu, and Jerry L Prince. Current methods in medical image segmentation. *Annual review of biomedical engineering*, 2(1):315–337, 2000.
- [2] Tao Lei, Risheng Wang, Yong Wan, Xiaogang Du, Hongying Meng, and Asoke K. Nandi. Medical image segmentation using deep learning: A survey. *ArXiv*, abs/2009.13120, 2022.
- [3] James S Duncan and Nicholas Ayache. Medical image analysis: Progress over two decades and the challenges ahead. *IEEE transactions on pattern analysis and machine intelligence*, 22(1):85–106, 2000.
- [4] Neeraj Sharma and Lalit M Aggarwal. Automated medical image segmentation techniques. *Journal of medical physics/Association of Medical Physicists of India*, 35(1):3, 2010.
- [5] KKD Ramesh, G Kiran Kumar, K Swapna, Debabrata Datta, and S Suman Rajest. A review of medical image segmentation algorithms. *EAI Endorsed Transactions on Pervasive Health and Technology*, 7(27):e6, 2021.
- [6] Nima Tajbakhsh, Jae Y Shin, Suryakanth R Gurudu, R Todd Hurst, Christopher B Kendall, Michael B Gotway, and Jianming Liang. Convolutional neural networks for medical image analysis: Full training or fine tuning? *IEEE transactions on medical imaging*, 35(5):1299–1312, 2016.
- [7] Erik Smistad, Thomas L Falch, Mohammadmehdi Bozorgi, Anne C Elster, and Frank Lindseth. Medical image segmentation on GPUs—a comprehensive review. *Medical image analysis*, 20(1):1–18, 2015.
- [8] Alberto Garcia-Garcia, Sergio Orts-Escolano, Sergiu Oprea, Victor Villena-Martinez, Pablo Martinez-Gonzalez, and Jose Garcia-Rodriguez. A survey on deep learning techniques for image and video semantic segmentation. *Applied Soft Computing*, 70:41–65, 2018.
- [9] Hang Yu, Laurence T Yang, Qingchen Zhang, David Armstrong, and M Jamal Deen. Convolutional neural networks for medical image analysis: State-of-the-art, comparisons, improvement and perspectives. *Neurocomputing*, 444: 92–110, 2021.
- [10] Le Cun Yan, B Yoshua, and H Geoffrey. Deep learning. *nature*, 521(7553):436–444, 2015.
- [11] Jonathan Long, Evan Shelhamer, and Trevor Darrell. Fully convolutional networks for semantic segmentation. In *Proceedings of the IEEE conference on computer vision and pattern recognition*, pages 3431–3440, 2015.
- [12] Panqu Wang, Pengfei Chen, Ye Yuan, Ding Liu, Zehua Huang, Xiaodi Hou, and Garrison Cottrell. Understanding convolution for semantic segmentation. In *2018 IEEE winter conference on applications of computer vision (WACV)*, pages 1451–1460. Ieee, 2018.
- [13] Shijie Hao, Yuan Zhou, and Yanrong Guo. A brief survey on semantic segmentation with deep learning. *Neurocomputing*, 406:302–321, 2020.
- [14] Mohammad Hesam Hesamian, Wenjing Jia, Xiangjian He, and Paul Kennedy. Deep learning techniques for medical image segmentation: achievements and challenges. *Journal of digital imaging*, 32(4):582–596, 2019.
- [15] Priyanka Malhotra, Sheifali Gupta, Deepika Koundal, Atef Zaguia, and Wegayehu Enbeyle. Deep neural networks for medical image segmentation. *Journal of Healthcare Engineering*, 2022.
- [16] Xiangbin Liu, Liping Song, Shuai Liu, and Yudong Zhang. A review of deep-learning-based medical image segmentation methods. *Sustainability*, 13(3):1224, 2021.
- [17] Nima Tajbakhsh, Laura Jeyaseelan, Qian Li, Jeffrey N Chiang, Zhihao Wu, and Xiaowei Ding. Embracing imperfect datasets: A review of deep learning solutions for medical image segmentation. *Medical Image Analysis*, 63:101693, 2020.
- [18] Olaf Ronneberger, Philipp Fischer, and Thomas Brox. U-Net: Convolutional networks for biomedical image segmentation. In *International Conference on Medical image computing and computer-assisted intervention*, pages 234–241. Springer, 2015.
- [19] Zongwei Zhou, Md Mahfuzur Rahman Siddiquee, Nima Tajbakhsh, and Jianming Liang. Unet++: Redesigning skip connections to exploit multiscale features in image segmentation. *IEEE Transactions on Medical Imaging*, 2019.
- [20] Fabian Isensee, Paul F Jaeger, Simon AA Kohl, Jens Petersen, and Klaus H Maier-Hein. nnu-net: a self-configuring method for deep learning-based biomedical image segmentation. *Nature methods*, 18(2):203–211, 2021.
- [21] Andrew J Ewald, Robert J Huebner, Hildur Palsdottir, Jessie K Lee, Melissa J Perez, Danielle M Jorgens, Andrew N Tauscher, Kevin J Cheung, Zena Werb, and Manfred Auer. Mammary collective cell migration involves transient loss of epithelial features and individual cell migration within the epithelium. *Journal of cell science*, 125(11):2638–2654, 2012.

- [22] Zongwei Zhou. *Towards Annotation-Efficient Deep Learning for Computer-Aided Diagnosis*. PhD thesis, Arizona State University, 2021.
- [23] Karen Simonyan and Andrew Zisserman. Two-stream convolutional networks for action recognition in videos. *Advances in neural information processing systems*, 27, 2014.
- [24] Leslie G Ungerleider and James V Haxby. ‘what’ and ‘where’ in the human brain. *Current opinion in neurobiology*, 4(2):157–165, 1994.
- [25] Chenyang Xu and Jerry L Prince. Gradient vector flow: A new external force for snakes. In *Proceedings of IEEE computer society conference on computer vision and pattern recognition*, pages 66–71. IEEE, 1997.
- [26] Michael Kass, Andrew Witkin, and Demetri Terzopoulos. Snakes: Active contour models. *International journal of computer vision*, 1(4):321–331, 1988.
- [27] Chenyang Xu and Jerry L Prince. Snakes, shapes, and gradient vector flow. *IEEE Transactions on image processing*, 7(3):359–369, 1998.
- [28] Liangliang Liu, Jianhong Cheng, Quan Quan, Fang-Xiang Wu, Yu-Ping Wang, and Jianxin Wang. A survey on u-shaped networks in medical image segmentations. *Neurocomputing*, 409:244–258, 2020.
- [29] Nahian Siddique, Sidike Paheding, Colin P Elkin, and Vijay Devabhaktuni. U-net and its variants for medical image segmentation: A review of theory and applications. *IEEE Access*, 2021.
- [30] Ozan Oktay, Jo Schlemper, Loic Le Folgoc, Matthew Lee, Mattias Heinrich, Kazunari Misawa, Kensaku Mori, Steven McDonagh, Nils Y Hammerla, Bernhard Kainz, et al. Attention u-net: Learning where to look for the pancreas. *arXiv preprint arXiv:1804.03999*, 2018.
- [31] Özgün Çiçek, Ahmed Abdulkadir, Soeren S Lienkamp, Thomas Brox, and Olaf Ronneberger. 3D U-net: learning dense volumetric segmentation from sparse annotation. In *International conference on medical image computing and computer-assisted intervention*, pages 424–432. Springer, 2016.
- [32] Róger Bermúdez-Chacón, Pablo Márquez-Neila, Mathieu Salzmann, and Pascal Fua. A domain-adaptive two-stream u-net for electron microscopy image segmentation. In *2018 IEEE 15th International Symposium on Biomedical Imaging (ISBI 2018)*, pages 400–404. IEEE, 2018.
- [33] Shaobo Min, Xuejin Chen, Zheng-Jun Zha, Feng Wu, and Yongdong Zhang. A two-stream mutual attention network for semi-supervised biomedical segmentation with noisy labels. In *Proceedings of the AAAI Conference on Artificial Intelligence*, volume 33, pages 4578–4585, 2019.
- [34] Zongwei Zhou, Md Mahfuzur Rahman Siddiquee, Nima Tajbakhsh, and Jianming Liang. Unet++: A nested u-net architecture for medical image segmentation. In *Deep Learning in Medical Image Analysis and Multimodal Learning for Clinical Decision Support*, pages 3–11. Springer, 2018.
- [35] <http://medicaldecathlon.com/>.
- [36] Melvyn A Goodale and A David Milner. Separate visual pathways for perception and action. *Trends in neurosciences*, 15(1):20–25, 1992.
- [37] Christoph Feichtenhofer, Axel Pinz, and Andrew Zisserman. Convolutional two-stream network fusion for video action recognition. In *Proceedings of the IEEE conference on computer vision and pattern recognition*, pages 1933–1941, 2016.
- [38] Eric Jang, Sudheendra Vijayanarasimhan, Peter Pastor, Julian Ibarz, and Sergey Levine. End-to-end learning of semantic grasping. In *Conference on Robot Learning*, pages 119–132. PMLR, 2017.
- [39] Berthold KP Horn and Brian G Schunck. Determining optical flow. *Artificial intelligence*, 17(1-3):185–203, 1981.
- [40] Deqing Sun, Stefan Roth, and Michael J Black. Secrets of optical flow estimation and their principles. In *2010 IEEE computer society conference on computer vision and pattern recognition*, pages 2432–2439. IEEE, 2010.
- [41] Yajie Xing, Jingbo Wang, Xiaokang Chen, and Gang Zeng. Coupling two-stream rgb-d semantic segmentation network by idempotent mappings. In *2019 IEEE International Conference on Image Processing (ICIP)*, pages 1850–1854. IEEE, 2019.
- [42] <https://www.creatis.insa-lyon.fr/Challenge/acdc/>.
- [43] <https://www.kaggle.com/c/data-science-bowl-2018>.
- [44] <http://pytorch.org/>.
- [45] Hongyi Wang, Shiao Xie, Lanfen Lin, Yutaro Iwamoto, Xian-Hua Han, Yen-Wei Chen, and Ruofeng Tong. Mixed transformer u-net for medical image segmentation. In *ICASSP 2022-2022 IEEE International Conference on Acoustics, Speech and Signal Processing (ICASSP)*, pages 2390–2394. IEEE, 2022.

-
- [46] Jieneng Chen, Yongyi Lu, Qihang Yu, Xiangde Luo, Ehsan Adeli, Yan Wang, Le Lu, Alan L Yuille, and Yuyin Zhou. Transunet: Transformers make strong encoders for medical image segmentation. *arXiv preprint arXiv:2102.04306*, 2021.
 - [47] Maxim Berman, Amal Rannen Triki, and Matthew B Blaschko. The lovász-softmax loss: A tractable surrogate for the optimization of the intersection-over-union measure in neural networks. In *Proceedings of the IEEE conference on computer vision and pattern recognition*, pages 4413–4421, 2018.
 - [48] Liang-Chieh Chen, Yi Yang, Jiang Wang, Wei Xu, and Alan L Yuille. Attention to scale: Scale-aware semantic image segmentation. In *Proceedings of the IEEE conference on computer vision and pattern recognition*, pages 3640–3649, 2016.
 - [49] Ashish Vaswani, Noam Shazeer, Niki Parmar, Jakob Uszkoreit, Llion Jones, Aidan N Gomez, Łukasz Kaiser, and Illia Polosukhin. Attention is all you need. *Advances in neural information processing systems*, 30, 2017.